

Propellant subsystem design for hypersonic cruiser exploiting liquid hydrogen

*Original*

Propellant subsystem design for hypersonic cruiser exploiting liquid hydrogen / Ferretto, D.; Fusaro, R.; Viola, N.. - ELETTRONICO. - (2022). ( AIAA Aviation 2022 Forum Chicago, IL (USA) 27/06/2022 - 01/07/2022) [10.2514/6.2022-3381].

*Availability:*

This version is available at: 11583/2971106 since: 2022-09-08T15:01:30Z

*Publisher:*

AIAA

*Published*

DOI:10.2514/6.2022-3381

*Terms of use:*

This article is made available under terms and conditions as specified in the corresponding bibliographic description in the repository

*Publisher copyright*

AIAA preprint/submitted version e/o postprint/Author's Accepted Manuscript

(Article begins on next page)

# Propellant subsystem design for hypersonic cruiser exploiting liquid hydrogen

D. Ferretto<sup>1</sup>, R. Fusaro<sup>2</sup> and N. Viola<sup>3</sup>

*Department of Mechanical and Aerospace Engineering*

*Politecnico di Torino*

*Corso Duca degli Abruzzi 24, Torino, 10129, Italy*

The possibility of establishing a new paradigm for commercial aviation towards high-speed flight in the next decades shall be inevitably preceded by the increase of Technology Readiness Level for those relevant enabling technologies associated to propulsion, thermal management and on-board subsystems, with particular attention also to environmental sustainability and economic viability of the proposed concepts. New design methodologies for both aircraft and on-board subsystems design shall then be based on holistic approaches able to catch the strong interactions between vehicle configuration, mission and subsystems architecture, which characterize high-speed aircraft layouts. This paper proposes a methodology for the preliminary sizing of propellant subsystems for liquid hydrogen powered hypersonic cruisers. Making benefit of traditional approaches, the process aims at introducing new design aspects directly connected to the peculiar multifunctional architecture of on-board subsystems for high-speed vehicles, so to be able to include additional analyses in early design stages, especially in case of high level of on-board integration. Notably, impact of requirements for Center of Gravity control, thermal, and, in general, energy management are considered as integral part of the method, with crucial implications on architecture selection. After the introduction of design algorithms for subsystem sizing, the STRATOFly MR3 hypersonic cruiser is taken as reference case study in order to provide a practical example of application of the proposed approach on a highly integrated platform.

## I. Nomenclature

$a$	=	major semi-axes of ellipsoidal tank section
$a_c$	=	radius of cylindrical tank section
$b$	=	minor semi-axes of ellipsoidal tank section
$d$	=	reference hydraulic diameter of the pipe
$g$	=	gravity acceleration
$h_{dome}$	=	tank dome height
$h_{fuel}$	=	heat of vaporization of the fuel
$k_{ins}$	=	thermal conductivity of tank insulation material
$l$	=	reference length of the pipe
$l_c$	=	length of cylindrical tank section
$n_x$	=	contingency factor due to manoeuvres
$p_1$	=	delivery pressure at pump station
$p_2$	=	delivery pressure at engine station
$p_p$	=	tank burst pressure

---

<sup>1</sup> Assistant Professor, Department of Mechanical and Aerospace Engineering, Politecnico di Torino

<sup>2</sup> Assistant Professor, Department of Mechanical and Aerospace Engineering, Politecnico di Torino

<sup>3</sup> Associate Professor, Department of Mechanical and Aerospace Engineering, Politecnico di Torino

$p_{tank}$	=	tank reference pressure
$p_v$	=	reference vapor pressure
$t_{flight}$	=	flight time
$t_{ins}$	=	thickness of tank insulation material
$t_{wshell}$	=	thickness of tank shell material
$v$	=	propellant speed in the ducts
$\epsilon$	=	absolute rugosity of pipes
$\eta$	=	efficiency
$\gamma$	=	specific weight of the propellant
$\lambda$	=	friction coefficient within the pipe
$\sigma_{ultimate}$	=	ultimate stress for tank shell material
$\rho_{fuel}$	=	propellant density
$\Delta p$	=	global pressure loss
$\Delta p_d$	=	distributed pressure loss
$\Delta p_c$	=	concentrated pressure loss
$\Delta p_g$	=	gravity pressure loss
$\Delta x$	=	difference in height between source and target propellant compartments
$B$	=	boil-off volume
$E_Y$	=	Young module of tank shell material
$K_c$	=	concentrated loss coefficient
$P$	=	pumping power
$\dot{Q}$	=	volumetric flow rate of propellant
$Re$	=	Reynolds number
$S$	=	safety factor
$T$	=	trapped fluid volume
$T_{fuel}$	=	reference propellant temperature
$T_{int}$	=	reference temperature for compartment adjacent to tank
$U$	=	ullage volume
$V$	=	fluid volume
$V_{tank}$	=	tank volume
$V_{tank_{eq}}$	=	equivalent tank volume (cylindrical section)
$V_{tank_{eq_{general}}}$	=	equivalent tank volume (ellipsoidal section)
$ATR$	=	Air Turbo Rocket
$CoG$	=	Center of Gravity
$CWT$	=	Center Wing Tank
$DMR$	=	Dual Mode Ramjet
$ECS$	=	Environmental Control Subsystem
$EPS$	=	Electrical Power Subsystem
$FAT$	=	Front Additional Tank
$FAT-FI$	=	FAT-Forward Intake
$FAT-FP$	=	FAT-Front Part
$FAT-MFP$	=	FAT-Middle-Front Part
$FAT-MP$	=	FAT-Middle Part
$FAT-MRP$	=	FAT-Middle-Rear Part
$FAT-RP$	=	FAT-Rear Part
$FCS$	=	Flight Control Subsystem
$FCU$	=	Fuel Control Unit
$FPT$	=	Front Pillow Tank
$FWT$	=	Front Wing Tank
$LAPCAT$	=	Long-term Advanced Propulsion Concepts And Technologies
$LH2$	=	Liquid Hydrogen
$MTOW$	=	Maximum Take-Off Weight

$(NPSH)_a$	=	Net Positive Suction Head available
<i>RPT</i>	=	Rear Pillow Tank
<i>RWT</i>	=	Rear Wing Tank
<i>STRATOFLY</i>	=	STRATOspheric FLYing opportunities for high-speed propulsion concepts
<i>TCS</i>	=	Thermal Control Subsystem
<i>TEMS</i>	=	Thermal and Energy Management Subsystem
<i>TRL</i>	=	Technology Readiness Level
<i>WTT</i>	=	Wing Tip Tank

## II. Introduction

The opportunity of reconsidering and re-introducing commercial high-speed flight has been firmly a recurring topic within the first half of the Twenty-First Century, since the decommissioning of Concorde. The need for a deep shift in aviation paradigm towards the reduction of flight time for long-haul routes urges designers to explore new solutions to improve the access to a world which keeps shrinking because of digitalization and business activities. On the other hand, the desire for a deeper human connection, especially in post-pandemic era, is expected to drive aviation industry demands in the next decades. Scientific community is thus assessing the potential of supersonic and hypersonic regimes to support feasible, sustainable and viable concepts of high-speed cruisers. In fact, an evolution of enabling technologies for high-speed flight, associated to propulsion, thermal management and on-board subsystems integration is a mandatory step to ensure vehicle feasibility, but it may be not enough to guarantee environmental sustainability and economic viability. In order to reach de-carbonization goals and climate impact levels scheduled for 2050 also in aviation domain, the selected technologies shall be characterized by a low environmental footprint, meeting conflicting requirements dealing with high performance and green aspects [1], [2]. Ultimately, vehicle concepts shall be viable and attractive from an economic perspective, being designed to be accessible and competitive on a very aggressive market [3]. The complexity related to these challenges can be very well understood by looking at the different initiatives spreading all over the world and dealing with high-speed flight research topics. Particularly, the work described in this paper has been carried out within the frame of H2020 Europe funded project STRATOFLY (STRATOspheric FLYing opportunities for high-speed propulsion concepts), conceived as a follow up of a series of European researches [4], which aims at studying the possibility of exploiting high-speed civil transportation systems at stratospheric altitudes, with the goal of reducing antipodal flight time of one order of magnitude with reference to conventional air transport, proposing a roadmap to reach Technology Readiness Level (TRL) of enabling technologies up to 6 by 2035 [5]. This includes, but is not limited to, the definition of new methodologies for aircraft configuration and on-board subsystems architecture design, the analysis of environmental impact of such kind of vehicles in terms of pollutant and noise emissions, as well as the economic and social assessments.

Notably, this paper deals with the definition of an integrated subsystems design methodology for hypersonic aircraft, with focus on propellant subsystem. This is surely one of the on-board subsystems which has the highest impact on vehicle configuration, because of the overall mass and volume allocated to the plant, as well as on the entire plants network on the aircraft, especially if cryogenic fluids are considered. In fact, the high complexity associated to the vehicle concept usually makes impossible to deal with individual design aspects separately, leading to the need of adopting methodologies capable of catching integration, interactions and interface issues among subsystems, as well as between subsystems network and vehicle layout. This is particularly applicable to propellant subsystem, which can be defined as a multifunctional plant on hypersonic aircraft platforms, embedding not only common functionalities associated to propellant storage and distribution (primary functions), but also additional capabilities linked to Center of Gravity (CoG) control and energy management (thermal control, environmental control). The level of integration of the different aspects is so high that the mission, the vehicle and the subsystems are strongly related to each other, thus a specific approach shall be considered to face the design.

This is a common point of most high-speed vehicle concepts, especially when flying in hypersonic regime, since on-board subsystems shall provide a resilient multi-functional architecture to effectively make benefit of the reduced volume available to face the issues produced by the hostile flight environment with the required level of performance.

Moreover, the use of cryogenic propellants, such as liquid hydrogen (LH2), offers the possibility not only to enhance the flight efficiency, because of the higher amount of energy per unit mass with reference to conventional

hydrocarbon fuels, but also the opportunity of supporting innovative thermal and, in general, energy management techniques [6], with implications on Thermal Control Subsystem (TCS), Environmental Control Subsystem (ECS) and Electrical Power Subsystem (EPS). Additionally, liquid hydrogen allows complete de-carbonization of flight (even if not yet of the overall supply chain), still posing, on the other hand, problems associated to storage (low energy per unit volume) and to water vapor emissions.

The paper describes the proposed methodology for propellant subsystem design in Section III, specifically dealing with a preliminary approach to cryogenic tanks design as well as to propellant distribution assembly characterization, highlighting the aspects associated to integration with other plants, vehicle and mission. Section IV proposes instead the application of the methodology to the STRATOFly MR3 case study, a liquid hydrogen powered hypersonic cruiser exploiting a waverider architecture and conceived to fly at around 35 km of altitude at Mach 8. Particularly, reference vehicle and mission are presented and, subsequently, an overview of tanks architecture and distribution assembly is provided. Overall subsystem physical breakdown in terms of mass, volume and power consumption is also reported. Ultimately, Section V draws major conclusions and suggests way forward.

### **III. Integrated Subsystems Design Methodology**

#### **A. Overview**

The proposed design methodology couples elements of the traditional propellant subsystems sizing approach [7] with peculiarities coming from the high-speed vehicles case study [8]. A summary of the process supporting the methodology is proposed in Fig. 1.

The first step consists in the analysis of mission requirements to evaluate the expected amount of fuel consumed during the flight. According to fuel type, a proper fluid volume can be computed and associated tanks volume breakdown (including also structural shell, supports and insulation) can be estimated, adopting simple correlations for tanks thickness evaluation for both structural and thermal aspects (Section III.B). It is worth highlighting that, at this stage, it is required to consider the constraints coming from vehicle configuration, defining equivalent tanks compartments (envelopes with equal volume but simplified shape) to be used as reference for the sizing process. Allocation of tanks on the vehicle layout can then start and the overall architecture shall take into account different aspects to produce an efficient solution, especially when dealing with cryogenic fluids. In fact, even if primary functionalities concerning storage and distribution shall be satisfied in the first place (positioning with reference to powerplant, mutual position of tanks etc...), propellants like liquid hydrogen can be used as an effective heat sink or coolant to reject heat fluxes produced during high-speed flight, so the position of tanks on-board can also be tailored to obtain the desired thermal environment within the aircraft. Additionally, tanks position and hierarchical classification (primary tanks for engine feed, secondary tanks etc...) can have a crucial impact on Center of Gravity (CoG) control during flight. Thus, a proper depletion sequence shall be identified and the hierarchical structure of compartments shall be studied in depth, together with the connections network of the pipes and of the pumping elements in order to meet performance requirements associated to mass flow and pressure levels. It is worth highlighting that the possibility of flying at a specific attitude, with a desired CoG position, can be crucial for high-speed vehicles, especially in hypersonic regime. In fact, these aircraft are characterized by a low aerodynamic efficiency [9], if compared to conventional airliners (only around 6-8 in cruise), being very susceptible to movable surfaces deflection for trim purposes (trim drag). CoG control through depletion sequence management can significantly enhance aerodynamic efficiency of the aircraft, by reducing deflections and related trim drag, allowing also to save fuel. Selection of transfer tanks and feed compartments is thus the core aspect of propellant tanks architecture definition.

Moreover, once the configuration is consolidated, the analysis of pressure and mass flow levels can be carried out, also evaluating pressure losses within the distribution lines to identify proper performance requirements for pumping elements, as function of engine parameters. The powerplant is in fact the driving element in the definition of distribution lines, since proper quantity of propellant shall be delivered at a specific pressure to ensure nominal operation. However, non-nominal scenarios shall be considered as well for redundancy reasons. It is thus clear that the selected depletion sequence shall satisfy performance requirements coming from the powerplant, the overall thermal management of the vehicle (hydrogen may be required to cool down aircraft elements), as well as from the requirements related to CoG control in flight. The overall set of operating parameters characterizing the behavior of the plant, especially considering active elements (those equipment which either consume or produce power) can be also fundamental to identify proper subsystem breakdown in terms of mass, volume and power consumption. In

fact, as last step of the iteration, the subsystem shall be characterized, at least from the point of view of the main elements, in terms of physical characteristics, that shall be compared with the related requirements in terms of practical possibility of sustaining the plant on-board. In case required volume and power consumption are within the limits offered by the configuration, as far as the overall subsystem mass is acceptable considering overall vehicle breakdown, the task can be considered completed. Otherwise, an iterative review of the subsystem is required, starting again from tanks sizing and allocation. In some cases, modifications to subsystem architecture may be enough to produce a feasible solution, while in specific scenarios, it may be required to trade some high-level requirements to reach convergence.

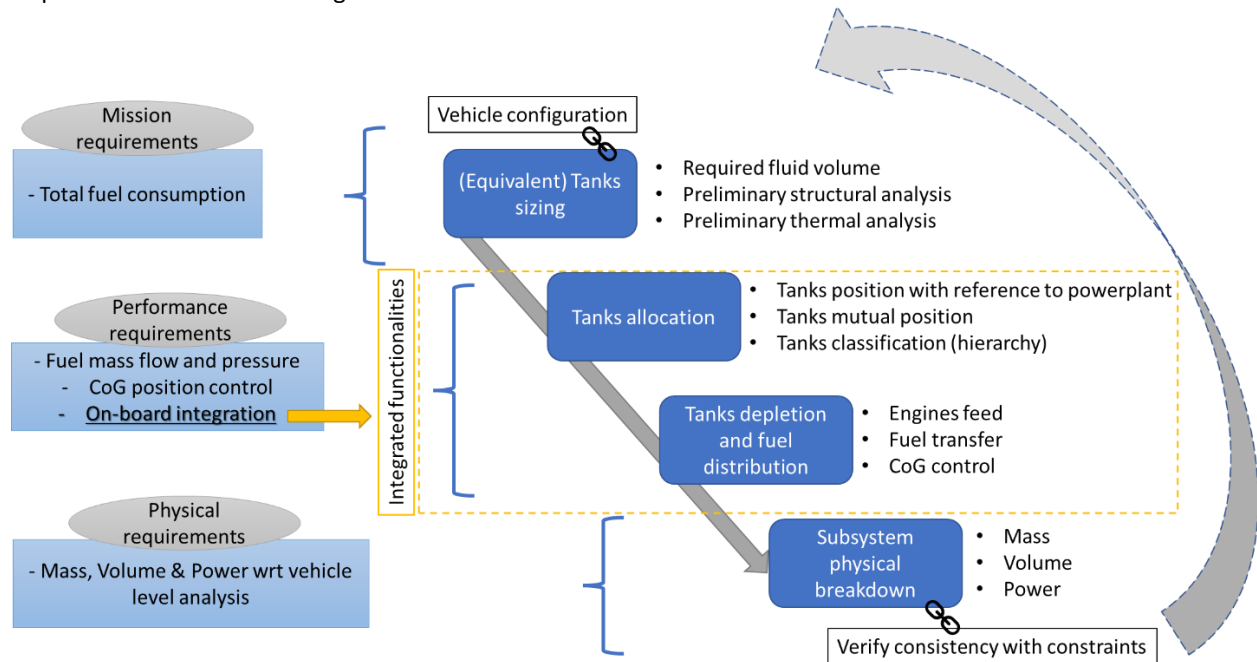


**Fig. 1 Overview of proposed propellant subsystems preliminary design methodology**

This qualitative description of the sizing process is quantitatively addressed for what concerns tanks and distribution assembly sizing in Sections III.B and III.C respectively. Peculiar aspects associated to CoG position control, as well as to issues related to other on-board subsystems integration, such as thermal management and on-board power generation, are faced directly within the analysis of the STRATOFly MR3 case study, since a specific configuration is required to perform the discussion.

## B. Preliminary cryogenic tanks design

Tanks are usually adopted to store liquid or gas propellant, guaranteeing proper values of pressure and temperature, allowing engine feed through the interface with distribution subsystems.

Depending on the type of propellant used, either storable or cryogenic, the design in terms of thermo-mechanical characteristics of the vessel can be different. Moreover, the shape of the tanks can vary as function of the type of application and of the space available within the vehicle. Typically it is possible to distinguish between integral tanks, usually adopted for aeronautical applications, where structure compartments themselves are used to store fuel, and rigid tanks, where separated and independent vessels are attached to the primary structure. As far as cryogenic applications are concerned, the rigid tanks architecture is the most used for obvious reasons. However, because of the uncertainties related to tanks shape, especially in early design stages, it is usually necessary to refer to equivalent cylindrical or well-known configurations to preliminarily identify structural and insulation thickness [8]. The model here presented makes in fact use of simple shapes to perform a parametrization of the tank, starting from a common volume.

A general expression for the propellant tank design volume [10] is reported in Eq. (1).

$$V_{tank} = V + T + B + U \quad (1)$$

Where

$V_{tank}$  is the tank design volume [ $m^3$ ]

$V$  is the actual volume of fluid required by the system [ $m^3$ ]

$T$  is the volume of fluid trapped within the system (not usable) [ $m^3$ ]

$B$  is the volume of fluid subjected to boil-off (only in case of cryogenic fluids) [ $m^3$ ]

$U$  is the ullage volume [ $m^3$ ]

Since the fluid volume is known, coming from mission requirements, it is possible to derive the design volume of the tank, which can be parametrized as an equivalent cylindrical tank (with elliptical domes), as reported in Eq. (2).

$$V_{tank_{eq}} = \pi a_c^2 l_c + \frac{4}{3} \pi a_c^2 h_{dome} \quad (2)$$

where

$a_c$  is the radius of the cylindrical section [m]

$l_c$  is the length of cylindrical section [m]

$h_{dome}$  is the height of the dome crown with respect to the end of cylindrical section [m]

Equation (2) can be generalized even more, by hypothesizing an ellipsoidal section for the cylindrical shape, with different semi-axes values, as reported in Eq. (3)

$$V_{tank_{eq_{general}}} = \pi a b l_c + \frac{4}{3} \pi a b h_{dome} \quad (3)$$

where

$a$  is the length of major semi-axis of the ellipsoidal section of the tank [m]

$b$  is the length of the minor semi-axis of the ellipsoidal section of the tank [m]

### 1. Structural design

The structural shell of the tanks shall be conceived to mainly withstand pressure loads coming from the internal compartments. Keeping in mind that structural materials for this kind of applications shall meet the required performance indexes in terms of strength over mass, fracture toughness and stiffness (low deformation) [11], also being characterized by low density and reduced permeation to liquids and gas, a well-established relation to iteratively estimate the minimum shell thickness can be defined as in Eq. (4) [12].

$$\frac{\sigma_{ultimate}}{S} \geq p_p \left( \left( \frac{a+b}{2t_{wshell}} \right) \left( 1 + 2 \left( 1 + 3.6 \frac{p_p}{E_\gamma} \left( \frac{a+b}{2t_{wshell}} \right)^3 \right) \left( \frac{a-b}{a+b} \right) \right) + \frac{1}{2} \right) \quad (4)$$

Where

$\sigma_{ultimate}$  is the ultimate stress for the selected material [Pa]

$S$  is a safety factor

$p_p$  is the burst pressure of the compartment [Pa]

$t_{wshell}$  is wall thickness of the shell [m]

$E_\gamma$  is the Young module of the material [Pa]

Surely, the selection of the material is a pre-requisite to identify a feasible architecture in terms of structural layout [4].

## 2. Thermal design

Passive insulation layers are usually selected in preliminary design stages to evaluate the required extra thickness and, also, extra amount of mass of the tank to meet thermal requirements. In fact, proper insulation is required to maintain temperature levels and gradients within acceptable limits, not only on fluid side, to reduce detrimental boil-off effects, but also on structure side, to avoid material embrittlement. Moreover, in case the propellant subsystem is highly integrated within the overall thermal management strategy of the vehicle, additional requirements may affect the design in terms of heat exchanges modulation. In general, even in presence of a multi-layered configuration for the insulating means or, also, in case of selection of a mixed active-passive layout, a first attempt to estimate the overall insulation amount required by tank assembly can be faced by relying on simple closed formulations making benefit of equivalent conductivities or heat exchange coefficients.

Similarly to what already described for structural thickness, the insulation thickness can be derived as in Eq. (5) [13], once mission parameters as well as interface temperature requirements are properly set.

This computation is applicable to cryogenic propellants, since storable propellants may not need a proper insulation.

$$t_{ins} = \sqrt{\frac{k_{ins} t_{flight} (T_{int} - T_{fuel})}{h_{fuel} \rho}} \quad (5)$$

Where

$\rho$  is the density of propellant [kg/m<sup>3</sup>]

$k_{ins}$  is the conductivity of insulation material [W/m K]

$t_{flight}$  is flight time [s]

$T_{int}$  is the temperature of the compartments adjacent to the tank (internal to the vehicle) [K]

$T_{fuel}$  is the temperature of the liquid inside the tank [K]

$h_{fuel}$  is the heat of vaporization of the fuel [J/kg]

Even if insulation contribution to overall mass may be reduced, because of the adoption of light materials and solutions, the impact on overall tank volume can be significant, since the thickness allocated to insulation layer can be an order of magnitude higher with respect to structural shell.

## C. Preliminary distribution assembly design

The characterization of distribution assembly in preliminary design stages is mainly aimed at identifying required power to drive pumping elements, as well as suction head limitations to avoid cavitation problems. The analysis shall be strictly linked to the allocation of tanks compartments on-board, since mutual positions, distance and attitudes may substantially affect the results, together with required performance in terms of delivery pressure and mass flow. The impact of vehicle configuration and mission profile (for nominal and non-nominal scenarios) is thus crucial to perform a consistent sizing process for the main distribution elements.

In general, the delivery pressure at pump  $p_1$  can be always computed as in Eq. (6), being function of desired pressure at the end of the circuit  $p_2$  and of pressure losses  $\Delta p$  acting along the path.

$$p_1 = p_2 + \Delta p \quad (6)$$

In turn, pressure losses  $\Delta p$  can be computed as the sum of distributed  $\Delta p_d$  and concentrated  $\Delta p_c$  losses, as well as gravity losses  $\Delta p_g$  as in Eq. (7-10).

$$\Delta p = \Delta p_d + \Delta p_c + \Delta p_g \quad (7)$$

$$\Delta p_d = \frac{1}{2} \rho v^2 \frac{l}{d} \lambda \quad (8)$$

$$\Delta p_c = \frac{1}{2} \rho v^2 K_c \quad (9)$$

$$\Delta p_g = n_x \gamma \Delta x \quad (10)$$

Where

$v$  is the fluid speed within the duct in  $\left[\frac{m}{s}\right]$

$l$  is the equivalent length of the duct in  $[m]$

$d$  is the hydraulic diameter of the duct in  $[m]$

$\lambda$  is the pressure loss coefficient

$K_c$  is the concentrated loss coefficient, simulating an equivalent duct with length representative of the actual loss

$n_x$  is contingency factor due to maneuvers in different directions

$\gamma$  is fluid specific weight in  $\left[\frac{N}{m^3}\right]$

$\Delta x$  is the difference in height or other directions between source and target compartment in  $[m]$

The pressure loss coefficient  $\lambda$  is function of Reynolds number and relative rugosity of the duct through the Moody diagram [14]. A good compromise to compute this value for different flow regimes is the so-called Haaland formulation [14], an explicit Colebrook-White model, as in Eq. (11).

$$\frac{1}{\sqrt{\lambda}} = -1.8 \log \left[ \left( \frac{\epsilon}{3.7d} \right)^{1.11} + \frac{6.9}{Re} \right] \quad (11)$$

Acceleration loads and maneuvers are taken from reference mission profile, together with required fuel flow to determine flow rate to be provided by pumping elements, as already mentioned. Overall, pumping power required  $P$  is a function of pump pressure and flow rate as simply reported in Eq. (12).

$$P = \frac{1}{\eta} p_1 \dot{Q} \quad (12)$$

Where

$\dot{Q}$  is the volumetric flow rate processed by the pump  $\left[\frac{m^3}{s}\right]$

$\eta$  is the efficiency for power conversion (from electrical/mechanical power to fluidic power)

Overall, pumping pressure shall also compliant with suction head limitations, so that the Net Positive Suction Head (NPSH) available, specified in Eq. (13) is higher than the required one.

$$(NPSH)_a = \frac{p_1 - p_v}{\rho g} = \frac{p_{tank} - p_v}{\rho g} + \Delta x - \frac{\Delta p}{\rho g} \quad (13)$$

Where

$p_{tank}$  is tank pressure in  $[Pa]$

$p_v$  is vapor pressure in  $[Pa]$

The determination of performance requirements associated to mass flow and pressure is particularly important in case of cryogenic propellant subsystems characterized by a high level of integration. In fact, requirements may come not only from the powerplant itself, usually defining proper rates and delivery pressure at Fuel Control Unit (FCU), but also from thermal management subsystems, for example in case a specific portion of fuel flow is used as coolant mean for additional users, as well as from power generation subsystems, in case the fluid is also adopted as main flow, within a thermodynamic cycle, to produce secondary power on-board [15].

Section IV shows a practical example of the implementation process for the design of a propellant subsystem being connected to other on-board plants and integrating functionalities for CoG control, thermal management and power generation, as studied within the STRATOFly Project [4].

## IV. STRATOFly MR3 case study

### A. Aircraft layout and reference mission

From the configuration standpoint, the STRATOFly MR3 aircraft follows the layout proposed by LAPCAT II Project for its MR2.4 vehicle [16], with some differences. It is characterized by a waverider architecture, with a dorsal-mounted propulsion plant duct, a canard and a V-Tail layout for directional stability and control. The main difference between MR2.4 and MR3 external layouts are related to the overall dimensions, which have been slightly extended for the MR3, the shape of the V-Tail, the upper part of the aft section of the nozzle, as well as the introduction of additional control surfaces (nozzle flaps). The integration of the propulsive system at the top of the vehicle allows maximizing the available planform for lift generation without additional drag penalties, thus increasing the aerodynamic efficiency, and it allows optimizing the internal volume. This layout guarantees furthermore to expand the jet to a large exit nozzle area without the need to perturb the external shape which would lead to extra pressure drag. Specifically, STRATOFly MR3 integrates 6 Air Turbo Rocket engines (ATR) that operate up to Mach 4-4.5 and one Dual Mode Ramjet (DMR) that is used for hypersonic flight from Mach 4.5 up to Mach 8.

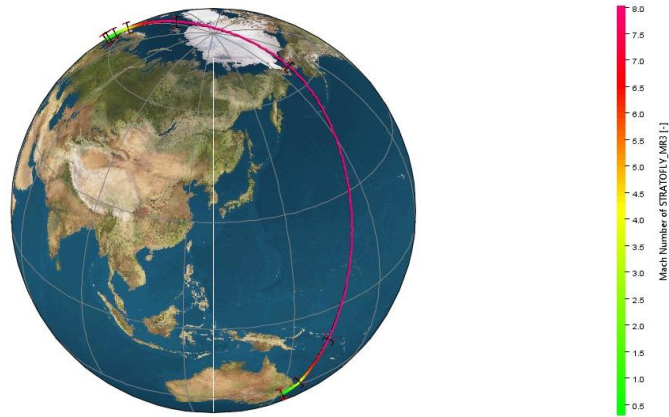


Fig. 2 The STRATOFly MR3 hypersonic cruiser

The external dimensions are characterized by an overall length of 94.7 m (excluding protruding rudders) and by a wingspan of 41.1 m. The planform area (excluding canards) is thus around  $2517 \text{ m}^2$  with an overall internal volume arrangement of roughly  $10000 \text{ m}^3$ . The vehicle is supposed to cover antipodal routes (19000 km), performing the cruise at stratospheric altitude (30-36 km) at Mach 8. The aircraft is designed to host 300 passengers as payload for the reference Brussels-Sydney mission. The propellant mass used is around 180000 kg of LH2 and the Maximum Take Off Weight (MTOW) is equal to 400000 kg. During the first part of the mission the ATR engines are used. The vehicle flies at subsonic speeds during the first phase, accelerating from Mach=0.37 to Mach=0.95 at an altitude between 11 km and 13 km. Then, the vehicle performs the subsonic cruise. This phase is needed to avoid the sonic boom while flying over land. The subsonic cruise phase ends when the vehicle is at 400 km from the departure

airport. During the next phase, the vehicle performs a second climb, until it reaches Mach 4 (supersonic climb). At the end of this phase, the ATR engines are switched off and the DMR is activated to accelerate up to Mach=8 at an altitude of 32-33 km (hypersonic climb). Here, the cruise starts at a constant Mach number of 8 and at an altitude between 32 and 36 km. During the first part of the cruise, the vehicle flies over the arctic region towards the Bering strait, between Asia and North America. Then, the vehicle continues to cruise over the Pacific Ocean towards Sydney. The cruise phase is over when a certain distance from the landing site is reached. This distance depends on the type of descent considered, i.e. powered or gliding descent.

The results of the reference trajectory simulation are reported in the following figures. The Brussels to Sydney mission can be completed with a total travel time of 3hr 24min. An overview of the complete trajectory is reported in Fig. 3 where the main characteristics of the trajectory can be clearly identified. The altitude and Mach profiles of the STRATOFLY MR3 vehicle are reported in Fig. 4 together with envisaged thrust profile, required to assure aeropropulsive balance to the aircraft over the entire mission, and with the trend associated to fuel consumption for both powerplants.



**Fig. 3 Overview of complete trajectory BRU-SYD. Trajectory is colored by Mach number**

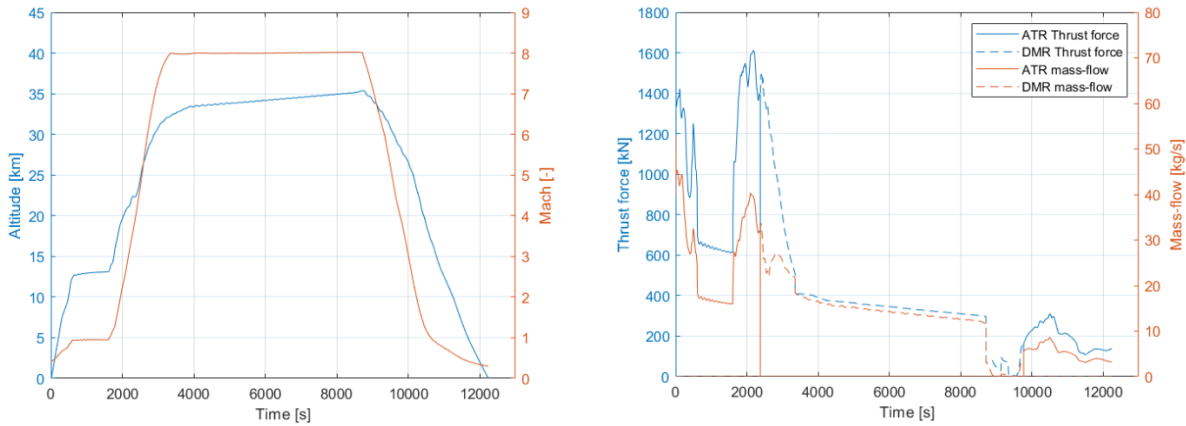


**Fig. 4 Altitude and Mach number vs Mission Time**

## B. Tanks architecture

The overall tanks architecture (Fig. 5) is made up of seven main assemblies that have been sized in terms of volume and thicknesses (both structural and insulation) in order to propose feasible bubbles layout, reducing structural loads and offering a good compromise between CoG control during flight as well as thermal management needs.

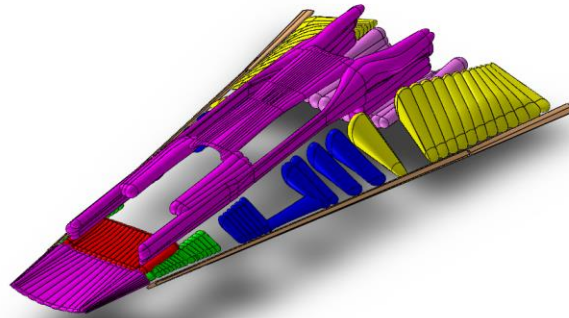


**Fig. 5 STRATOFly MR3 propellant tanks layout**

The vehicle has an overall tanks volume of  $2353 \text{ m}^3$  and is able to host around  $2117 \text{ m}^3$  of LH2 (90% tanks efficiency), corresponding to  $141440 \text{ kg}$  of fluid in case of a density equal to  $70.72 \text{ kg/m}^3$  (with a temperature of 20 K). If density of LH2 is increased to  $90 \text{ kg/m}^3$  (with a temperature of 13 K) the total mass of fluid can reach  $180000 \text{ kg}$ , as required by the nominal mission. In this case, a 5% margin on propellant mass is also taken into account.

The main tanks assemblies, depicted in Fig. 5, are listed hereafter:

- Front Additional Tank (FAT) assembly, constituted by a front part, close to the intake, and by a main part all along aircraft fuselage (dark purple);
- Front Pillow Tank (FPT) assembly, which has a single compartment close to the front part of the FAT (red);
- Front Wing Tank (FWT) assembly, which is located along the leading edge of the wing in the front part (green);
- Center Wing Tank (CWT) assembly, which is positioned in the middle of wing compartments (blue);
- Rear Wing Tank (RWT) assembly, which is the bigger among wing tanks assemblies, located in the aft region of the wing, almost up to the trailing edge (yellow);
- Rear Pillow Tank (RPT) assembly, which has a single compartment at the bottom of 3D nozzle in the aft fuselage area of the aircraft (light purple);
- Wing Tip Tank (WTT) assembly, which is a thin compartment positioned all along wing leading edge (orange).

Tanks have been preliminary sized for what concerns both structural and thermal aspects using the correlations shown in Section III.B. Structural breakdown has also been detailed through proper optimization process [17] which is out of scope for this paper. However, in order to maintain consistency with the final layout of the tanks, these refined values are shown in Table 1. Pressure has been considered equal to 1 bar, while input coming from a preliminary thermal analysis [18] was used to manage thermal requirements for the tanks (internal temperature of the fluid 13 – 20 K). Structural material is Aluminum 7075, while passive insulation is based on low conductivity plastic fibers.

**Table 1 Tanks characteristics for STRATOFly MR3**

Tank assembly	Fluid volume [m3]	Fluid mass [kg] @13K	Tank shell thickness [m]	Tank insulation thickness [m]
FAT	836	75241	0.03	0.115
FPT	125	11291	0.010	0.115
FWT (B4)	30	2735	0.040	0.115
CWT (B)	198	17806	0.040	0.108
RWT (B2)	616	55374	0.013	0.115

RPT	294	26454	0.005	0.115
WTT	18	1624	0.005	0.015

Main assemblies have also been divided in low level compartments (Fig. 6), so to instantiate a hierarchical distribution strategy, as indicated in Section IV.C.

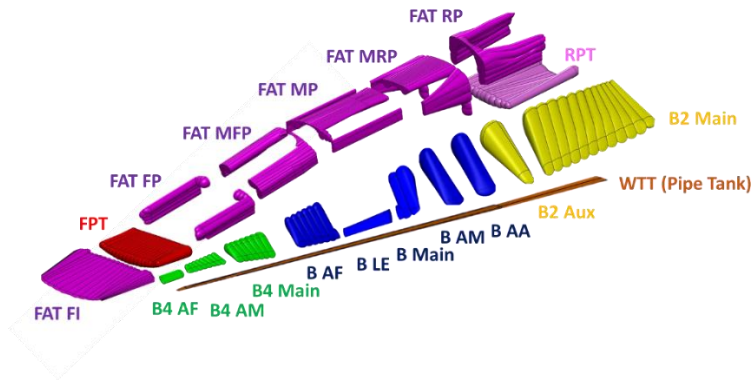


Fig. 6 STRATOFly MR3 propellant sub-compartments

### C. Distribution assembly architecture and analysis of depletion sequence

The analyses shown in Section IV.A concerning mission simulation allowed establishing the reference fuel flow profile for both ATR and DMR engines. This is the main driver for the identification of engine feed sequence and performance from the point of view of the propellant subsystem. However, as already highlighted, additional considerations concerning CoG positions during the flight, which is highly connected to stability and controllability of the aircraft, shall be taken into account while defining the reference depletion sequence. In fact, some guidelines concerning best CoG positions to be maintained during flight have been generated from mission and Flight Control Subsystem (FCS) analyses, in order to guarantee stability and to reduce deflections of mobile surfaces, enhancing lift-over-drag ratio of the aircraft by minimizing trim drag. As baseline, Fig. 7 shows the best CoG positions in terms of deflections of nozzle flaps as function of Mach number [19]. This is an index for the overall set of movable surfaces of the MR3, since the level of deflection of nozzle flaps required for controllability is similar to the amount allocated to other surfaces for longitudinal control (e.g. canard and elevons). This means that the “green zone” allows reducing the trim drag, since deflections are minimized, being preferable to fly in these conditions, where possible. Tanks depletion sequence shall then focus on controlling CoG so to stay as much as possible in this area.

LEGEND		CoG position - Climb/Cruise											
$\delta_{body/flap}$		53	52.5	52	51.5	51	50.5	50	49.5	49	48.5	48	
0	Mach	0.3	-30	-25	-25	-25	-25	-20	-20	-20	-10	0	
-5		0.5	-30	-25	-25	-25	-25	-20	-20	-20	-10	0	
-10		0.7	-25	-25	-25	-20	-20	-20	-10	0	0	0	
-15		0.8	-25	-25	-25	-20	-20	0	0	0	0	0	
-20		0.95	-20	-20	-20	-15	0	0	0	0	0	0	
-25		1.05	-25	-20	-20	0	0	0	0	0	0	0	
-30		1.2	-25	-20	-20	0	0	0	0	0	0	0	
		1.5	-25	-25	-20	-20	-20	0	0	0	0	-10	-10
		1.7	-25	-25	-25	-20	-20	-20	-15	-10	-10	-10	-10
		2	-25	-25	-25	-20	-20	-20	-20	-15	-10	-10	-10
		3	-25	-25	-25	-25	-25	-20	-20	-20	-20	-20	-15
		4	-25	-25	-25	-20	-20	-20	-15	-15	-10	0	0
		5	-25	-25	-25	-20	-20	-20	-15	0	0	0	0
		6	-25	-25	-20	-20	-20	-20	-15	-15	0	0	0
		7	-25	-25	-20	-20	-20	-20	-15	0	0	0	0
		8	-25	-25	-20	-20	-20	-20	-15	-15	-15	-10	0

Fig. 7 Expected deflections for nozzle flaps as function of Mach number and CoG positions

From these data, a reference CoG profile, guaranteeing minimum trim drag has been defined, as reported in Fig. 8, as function of mission time and Mach number.

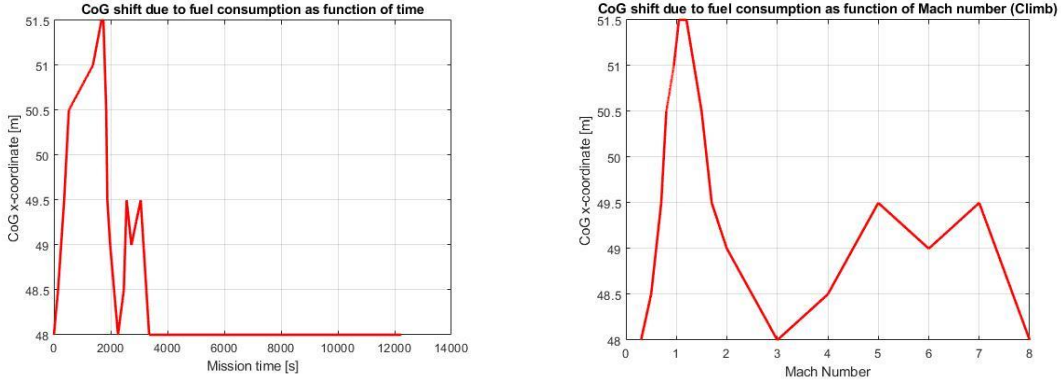


**Fig. 8 Reference CoG profile for trim drag minimization as function of mission time (left) and Mach number (right, for climb only)**

Then, the analysis of tanks compartments, described in previous sections, led to the identification of a suitable depletion sequence, as reported in Fig. 9. The sequence starts with the aft compartments, so to move the CoG forward as fast as possible, reaching lower deflections for the movable surfaces (RPT and RWT are depleted). Then, a more detailed CoG control is performed also looking at the profile specified in Fig. 9 (left). In this case, front part of FAT, as well as FPT, FWT and CWT compartments are depleted. In the end, rear FAT compartments and main tanks are progressively emptied, together with WTT. The right side of Fig. 9 shows instead the remaining propellant within main tanks assemblies, as consequence of compartments depletion.

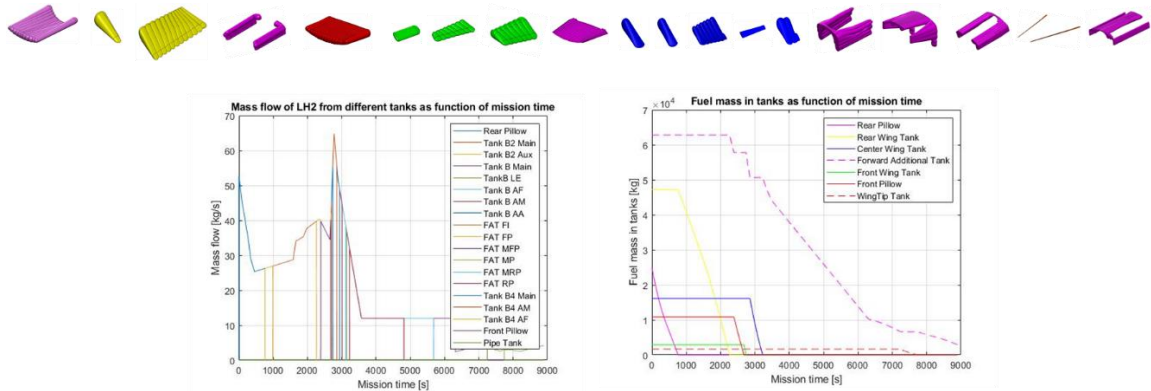


**Fig. 9 STRATOFly MR3 fuel tanks depletion sequence (legend does not follow depletion order)**

It is not possible to completely follow the profile shown in Fig. 8, especially at the beginning of the mission (when the vehicle is fully loaded with propellant and it is not physically possible to meet CoG profile up to a certain depletion percentage) and during some acceleration legs. Figure 11 reports the effect of the actual depletion profile in terms of CoG displacement.

		CoG position - Climb/Cruise										
		53	52.5	52	51.5	51	50.5	50	49.5	49	48.5	48
Mach	0.3	-30	-25	-25	-25	-25	-25	-20	-20	-20	-10	0
	0.5	-30	-25	-25	-25	-25	-20	-20	-20	-10	0	0
	0.7	-25	-25	-25	-20	-20	-20	-10	0	0	0	0
	0.8	-25	-25	-25	-20	-20	0	0	0	0	0	0
	0.95	-20	-20	-20	-15	0	0	0	0	0	0	0
	1.05	-25	-20	-20	0	0	0	0	0	0	0	0
	1.2	-25	-20	-20	0	0	0	0	0	0	0	0
	1.5	-25	-25	-20	-20	-20	0	0	0	0	-10	-10
	1.7	-25	-25	-25	-20	-20	-20	-15	-10	-10	-10	-10
	2	-25	-25	-25	-20	-20	-20	-20	-15	-10	-10	-10
	3	-25	-25	-25	-25	-25	-25	-20	-20	-20	-20	-15
	4	-25	-25	-25	-20	-20	-20	-15	-15	-10	0	0
5	-25	-25	-25	-20	-20	-20	-15	0	0	0	0	
6	-25	-25	-20	-20	-20	-20	-15	-15	0	0	0	
7	-25	-25	-20	-20	-20	-20	-15	0	0	0	0	
8	-25	-25	-20	-20	-20	-20	-15	-15	-15	-10	0	

Fig. 10 Position of CoG and effect on deflections as function of selected fuel depletion sequence

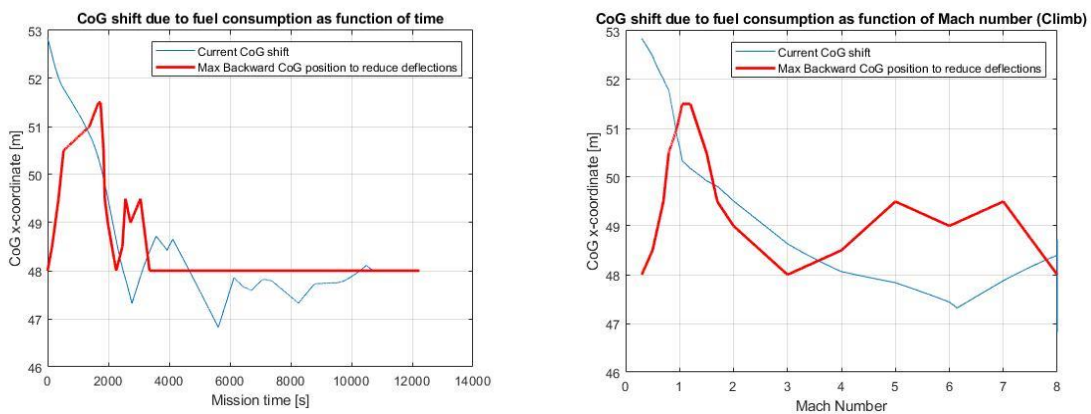
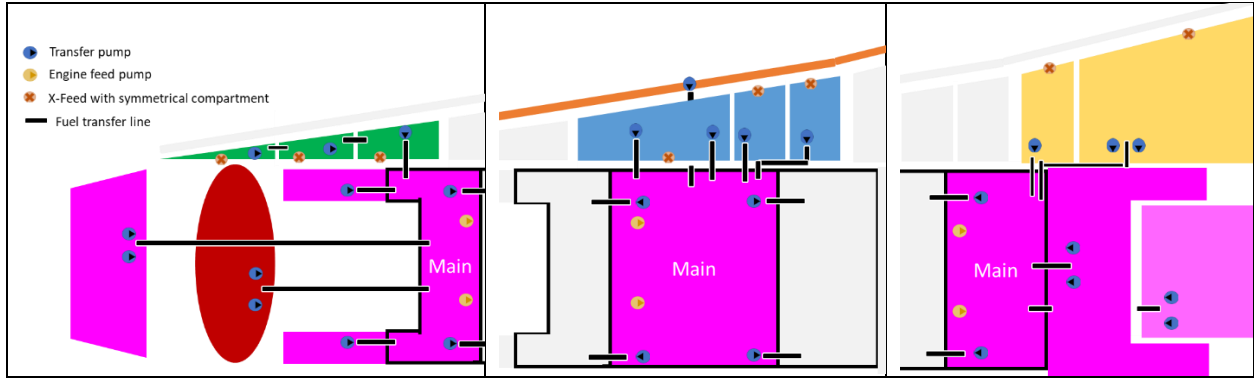


Fig. 11 Actual CoG displacement as function of selected fuel depletion sequence vs reference profile as function of time (left) and of Mach number (right, for climb only)

This is a preliminary study aimed at identifying suitable concepts for propellant management on-board, thus a refinement of the sequence, also adopting detailed control devices, may increase the efficiency of the procedure. It is important to highlight that, in order to minimize deflections, the blue line reported in Fig. 11 shall be below the red one, i.e. the CoG position corresponding to the actual sequence shall be closer to aircraft leading edge than the one specified by the reference profile all along the mission. As already mentioned, critical points are present at the beginning of the flight, as well as during acceleration and at the beginning of the cruise. In any case, with reference to the overall mission, these phases are limited in time, being only 25% of flight time.

Once the depletion sequence is identified, it is possible to finalize tanks architecture and hierarchical arrangement on-board. This allows the identification of main pumping elements as well as of the main connections between the tanks, also considering non-nominal scenarios. Particularly, Fig. 12 (left) shows the layout of tanks in the front part of the aircraft. The primary tank of the assembly is the FAT-MFP which has two engine feed pumps and two transfer circuits, connecting it respectively to powerplant and FAT-MP. FAT-FI and FPT auxiliary tanks are connected to FAT-MFP by means of two transfer pumps each. FWT compartments are connected to FAT-MFP through a transfer pump in the bigger compartment, while smaller ones are connected in sequence. Possibility of performing cross-feed between left-hand and right-hand sides of FWT is present for each compartment. Ultimately, FAT-FP compartments are connected to FAT-MFP through one transfer pump per side.



**Fig. 12 Tanks architecture layout of the STRATOFly MR3**

Figure 13 (centre) shows the layout for central area of the aircraft. In this case, the FAT-MP is the primary tank, which is connected to powerplant by means of two delivery pumps, as well as to FAT-MFP and FAT-MRP through two transfer pumps. CWT and WTT are auxiliary tanks. CWT compartments are directly connected to the primary tanks by means of transfer pumps and, particularly, the main compartment of CWT, which is an assembly of three parts, allows internal movement of the fluid. This has two transfer pumps, while other compartments have only one. The WTT is directly connected to FAT-MP as well by means of a transfer pump. The compartments of CWT can communicate with symmetrical ones by means of dedicated cross-feed valves, while this option is not included for WTT.

Ultimately, Fig. 12 (right) shows the layout at rear part of the aircraft. The FAT-MRP is the primary tank, whilst RWT, RPT and FAT-RP are auxiliary tanks. The primary tank is connected to powerplant by means of two delivery pumps, and to FAT-MP through two transfer pumps. All other compartments of auxiliary tanks are directly connected to FAT-MRP by means of two transfer pumps each, except for the smaller compartment of RWT which has a single pump. Right-hand and left-hand side of RWT can be connected through proper cross-feed channels. Pumping power has been then computed for the different compartments, separating transfer power from engine feed related power. Results are shown in Fig. 13.

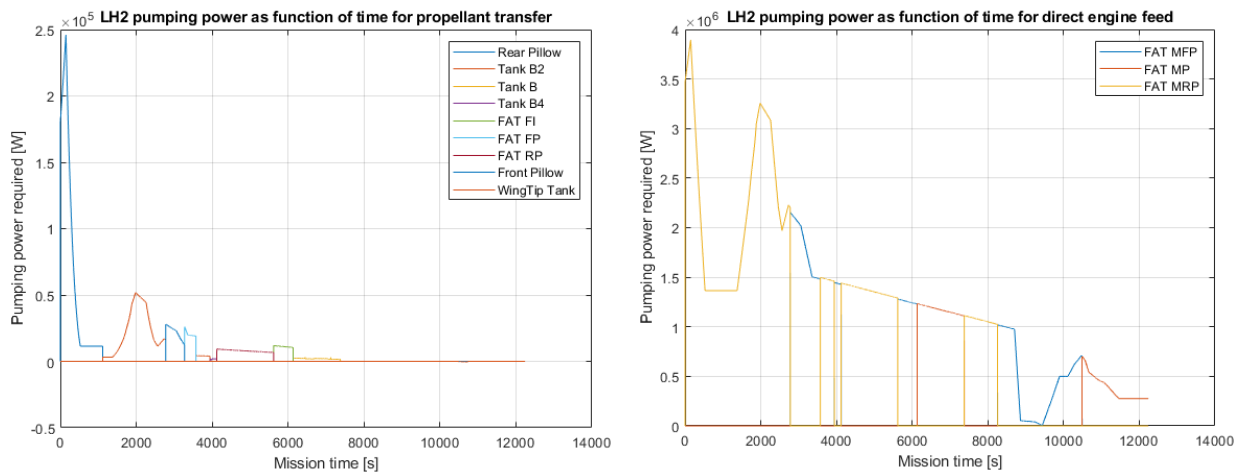


**Fig. 13 Overview of pumping power due to propellant transfer (left) and engine feed (right) for STRATOFly MR propellant subsystem**

As it can be seen, the high pressure at FCU (60 bar have been hypothesized for injection) causes a very high pumping power for engine feed, whilst transfer power is instead easily manageable. The peak for engine feed pumping power is around 3.7 MW, while transfer power has an average value of 25 kW with a peak very limited in time which is an

order of magnitude higher. RPT transfer pumps are assumed to require a high amount of power in the initial phases of the flight (the amount of fuel that shall be transferred to FAT-MRP is high since powerplant requires a high mass flow). However, additional contributions to the initial transfer may come from FAT-RP as well as from RWT compartments in order to guarantee a short time boost with low impact on overall depletion sequence and a reduced influence on expected CoG displacement.

While transfer pumps can be electrically-driven, the high power level required for engines feed pumps does not allow the selection of electrical feed machines for these applications.

#### D. Subsystem physical breakdowns

With all relevant information regarding tanks and pumping machines, it is possible to proceed through physical breakdown computation. Particularly, for what concerns tanks, it is straightforward to compute the overall mass since this is directly proportional to the previously computed thicknesses. The mass breakdown is shown in Table 2.

**Table 2 Tanks mass breakdown (empty mass)**

Tank	Mass [kg]
Front Additional Tank (FAT)	23018
Front Pillow Tank (FPT)	3976
Forward Wing Tank (FWT)	500
Center Wing Tank (CWT)	5913
Rear Wing Tank (RWT)	17310
Rear Pillow Tank (RPT)	1097
Wing Tip Tank (WTT)	150
<b>Total</b>	<b>51964</b>

Electrical pumps for propellant transfer and turbopumps for engines feed can be sized looking at the main operating parameters (performance indexes) as well as at some configuration features which depend on the type of machine being selected. As suggested in [6] and [20], for example, it is possible to compute physical breakdowns of these machines once mass flow, fluid characteristics, pressure and head are known. Considering the architecture sketched in Section IV.C, the propellant subsystem of STRATOFly MR3 requires 40 electrical transfer pumps and 6 turbopumps for engine feed, as reported in Table 3.

**Table 3 Physical breakdown of pumping elements**

Element	Number	Total Mass [kg]	Total Volume [m <sup>3</sup> ]
Transfer pump	40	1100	0.20
Feed turbopump	6	870	0.15
<b>Total</b>	<b>46</b>	<b>1970</b>	<b>0.35</b>

A provisional summary for the overall physical breakdown of propellant subsystem is provided in Table 4, where pipes contribution is not included. This can be a considerable portion of the breakdown so proper margin policies should be adopted at this stage of design [21].

**Table 4 Overall subsystem breakdown**

Assembly	Mass [kg]	Volume [m <sup>3</sup> ]
Propellant transfer pumps	1100	0.20
Engine feed turbopumps	870	0.15
Tanks	51964	2353
<b>Total</b>	<b>53934</b>	<b>2353.35</b>

#### E. Additional implications of integrated on-board subsystems architecture for the case study

Section IV.C is mainly based on the sizing of the subsystem looking at powerplant and CoG requirements. However, as already anticipated, LH2 can be efficiently used as driving fluid for cooling purposes before entering the combustion chamber of the powerplant. The adoption of regenerative cooling techniques with integrated power

generation capabilities [22], [23] is a common topic in hypersonic vehicles design campaigns. Notably, the STRATOFly MR3 is conceived to host a dedicated Thermal and Energy Management Subsystem (TEMS), responsible for secondary power generation on-board (to feed the different electrical utilities) when the powerplant is running in ramjet/scramjet modes (i.e., when powerplant does not allow for gearboxes connections, not featuring movable parts). This guarantees the self-sustainment of the vehicle in high-speed flight, avoiding the need of oversizing dedicated batteries and assuring a re-use of the boil-off generated within the tanks. At the same time, the use of LH2 to collect heat from the airframe and the powerplant itself, before the injection in the combustor, allows to save energy, enhancing the specific fuel consumption of the overall concept. The original TEMS architecture studied within LAPCAT II Project [15], exploited LH2 within a regenerative cooling cycle to cool down powerplant elements (especially combustion chambers and nozzle through a cooling jacket architecture), using the fluid from the engine feed line. This fluid, pumped through dedicated components, is then heated and subsequently expanded through a turbine before the injection within the combustor. On the other hand, the boil-off produced within the LH2 tanks can be used in parallel as additional coolant mean for other elements of the aircraft (such as ECS heat exchangers, cabin etc...), being compressed through a dedicated machine driven by the LH2 turbine. Excess of power, generated through the expansion within the turbine can be used for other on-board needs, exploiting proper generators connected to the turbomachinery shaft. The STRATOFly MR3 TEMS concept has a similar architecture, being based on the same physical phenomena. However, a higher level of details for what concerns the operational configuration has been devoted to implement a feasible solution within the aircraft, overcoming the pure theoretical concept and sketching the interfaces with the new on-board subsystems architecture. The basic cycle of the updated TEMS is reported in Fig. 14. As it can be seen, the LH2 line (blue) is used within the regenerative cooling cycle on the powerplant, collecting the LH2 from auxiliary tanks (through transfer pumps), delivering it to the primary tank and then to the dedicated engine cooling jackets. After the heating, the fluid is expanded through a turbine, which cools down the hydrogen, setting also the correct injection pressure, and produces power to drive other TEMS utilities, as well as to feed other on-board subsystems through dedicated generators, if required. Main pumping assembly can be driven by the TEMS turbine itself, considering the high-power demand (Section IV.C). The boil-off line (cyan) is instead dedicated to cooling of other utilities and loads. The gaseous hydrogen is collected from the different tanks and compressed in order to be injected within a dedicated cycle. The boil-off compressor is driven by the LH2 turbine. Once the boil-off has concluded its cycle, it is injected within the powerplant, by mixing with LH2 line after the turbine.

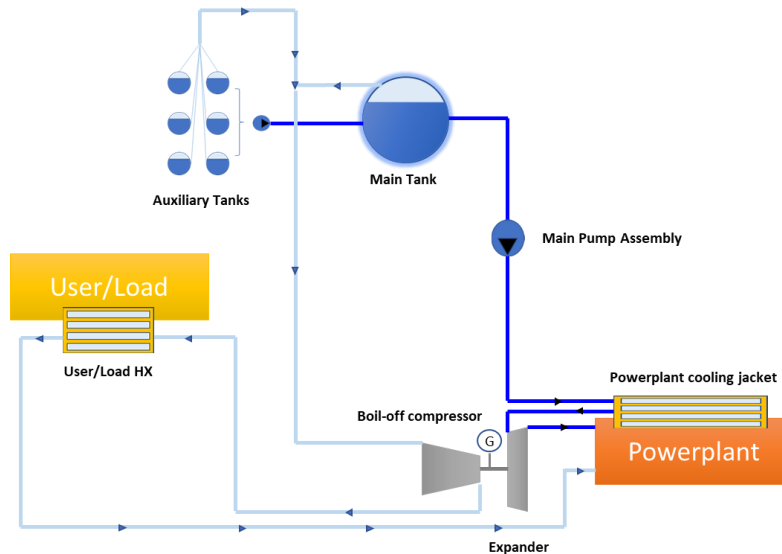


**Fig. 14 TEMS cycle architecture**

The TEMS is crucial for high-speed flight phases, but it can be exploited also for slower regimes, since it can be theoretically operated even with ATR, if engines are running (an hydrogen flow through the turbine is required, so pumps shall be active), reducing the power bleed from the powerplant and, as consequence, reducing the fuel

consumption. For these reasons, in order to allocate this TEMS concept on-board and to connect it to the operational modes of powerplant and other subsystems, a dedicated analysis was carried out to translate the theoretical cycle in a implemented schematic. In fact, considering the layout of the aircraft and, particularly, the propellant depletion sequence defined in Section IV.C, the TEMS has been divided in three modules (front, centre and rear). This subdivision is necessary to allow connection of TEMS with the three different primary tanks (and related auxiliary compartments), in order to allow a complete coverage of mission phases, in terms of cooling and power generation capabilities, considering that the delivery line shall be active to guarantee nominal operation of the plant. At the same time, all modules are connected to main users, such as ECS and powerplant cooling jacket, in order to assure seamless operation during the switch between one module and another one. Moreover, the presence of different modules may allow to enhance the operational safety, since possible failures, especially within delivery lines, leading to cooling or power generation problems, can be balanced by other modules of TEMS. Additionally, the different modules, depending on their position on-board (front part, middle part, aft part of the aircraft) can deal with local utilities requirements in terms of cooling, and offer a more flexible solution for the real-life implementation on-board with reference to the single plant, which can result difficult to install in one shot. Analysis of the performance of such type of cycle shall be performed through detailed simulations to assess the behaviour of turbomachinery elements in subsequent design stages, especially looking at temperature and power levels at the different locations of the plant.

## V. Conclusion

This paper presented a methodology for the preliminary design of a cryogenic propellant subsystem for hypersonic flight applications. The overall process included the definition of relevant mission and performance requirements impacting the sizing rationale, the characterization of tanks and the allocation of the compartments on-board, the definition of propellant distribution assembly and the evaluation of physical breakdowns of the plant. The methodology was specifically conceived to provide an integrated view over the mutual influences of different on-board subsystems within the vehicle architecture, so to highlight the need of moving from a standalone approach to an holistic paradigm, especially when dealing with configurations of aircraft featuring a high degree of complexity. The application of the methodology to the STRATOFly MR3 concept, a Mach 8 hypersonic waverider for passengers transportation exploiting liquid hydrogen, was used to demonstrate the implications of the approach on a specific case study. In this context, the sizing of tanks and pumping elements of the distribution subsystem was performed, looking at additional functionalities allocated on propellant subsystem (other than the obvious ones associated to propellant storage and supply) such as CoG and thermal control. For this reason, a concept for integrated on-board energy management has been suggested in order to simultaneously satisfy the requirements coming from aerodynamic analysis (with the aim of minimizing the trim drag) as well as from energy assessment (assuring temperatures control, secondary power self-sustainment in high-speed flight and fail safe architecture needs). The derived integrated subsystems architecture shall be subjected to further analyses, in order to assess the behavior of main components through simulation, in order to identify potential refinements to the concept during subsequent design stages.

## Acknowledgments

This work has been carried out within the frame of “STRATOspheric FLYing opportunities for high-speed propulsion concepts” (STRATOFly) project. This project has received funding from the European Union’s Horizon 2020 research and innovation program under grant agreement No 769246.

## References

- [1] Fusaro, R., Viola, N. and Galassini, D., “Sustainable Supersonic Fuel Flow Method: an Evolution of the Boeing Fuel Flow Method for Supersonic Aircraft Using Sustainable Aviation Fuels”, *Aerospace*, Vol. 8, N. 331, 2021.  
<https://doi.org/10.3390/aerospace8110331>
- [2] Fusaro, R., Vercella, V., Ferretto, D., Viola, N. and Steelant, J., “Economic and environmental sustainability of liquid hydrogen fuel for hypersonic transportation systems”, *CEAS Space Journal*, Vol. 12, 2020, pp. 441-462.  
<https://doi.org/10.1007/s12567-020-00311-x>

- [3] Margaretic, P. and Steelant, J., "Economical assessment of commercial high-speed transport", *CEAS Aeronautical Journal*, Vol. 9, 2018, pp. 747-764.  
<https://doi.org/10.1007/s13272-018-0319-y>
- [4] Viola, N., et al., "H2020 STRATOFly Project : from Europe to Australia in less than 3 hours", *32<sup>nd</sup> Congress of the International Council of the Aeronautical Sciences*, Shanghai, CN, 2021.
- [5] Vercella, V., Fusaro, R and Viola, N., "Technology roadmaps for the development of future high-speed transportation systems", *32<sup>nd</sup> Congress of the International Council of Aeronautical Sciences, Shanghai*, CN, 2021.
- [6] Fusaro, R., Ferretto, D., Viola, N., Fernandez Villace, V., and Steelant, J., "A methodology for preliminary sizing of a Thermal and Energy Management System for a hypersonic vehicle", *The Aeronautical Journal*, Vol. 123, N. 1268, 2019, pp. 1508 – 1544.  
<https://doi.org/10.1017/aer.2019.109>
- [7] Langton, R., Clark, C., Hewitt, M., and Richards, L., *Aircraft Fuel Systems*, Aerospace Series, edited by I. Moir, A. Seabridge and R. Langton, John Wiley & Sons, Chichester, UK, 2009, pp. 19 – 29.
- [8] Fusaro, R., and Viola, N., "Design and integration of a cryogenic propellant subsystem for the hypersonic STRATOFly MR3 Vehicle", *AIAA Scitech 2020 Forum*, 2020, pp. 1106 – 1118.  
<https://doi.org/10.2514/6.2020-1106>
- [9] Viola, N., Roncioni, P., Gori, O., and Fusaro, R., "Aerodynamic Characterization of Hypersonic Transportation Systems and Its Impact on Mission Analysis", *Energies*, Vol. 14, N. 3590, 2021.  
<https://doi.org/10.3390/en14123580>
- [10] Dieter, D. K., and Huang, D. H., "Modern engineering for design of liquid-propellant rocket engines", *Progress in Astronautics and Aeronautics*, Vol. 147, AIAA, 1992.
- [11] Ashby, M. F., "Materials selection in mechanical design", 2<sup>nd</sup> ed., Butterworth Heinemann, Oxford, UK, 1999, Chaps. 5, 6.
- [12] Winnefeld, C., Kadyk, T., Bensmann, B., Krewer, U., and Hanke-Rauschenbach R., "Modelling and Designing Cryogenic Hydrogen Tanks for Future Aircraft Applications", *Energies*, Vol. 11, N. 105, 2018.  
<https://doi.org/10.3390/en11010105>
- [13] Ardema, M. D., "Solutions of Two Heat-Transfer Problems with Application to Hypersonic Cruise Aircraft", NASA TM X-2025, 1970.
- [14] Massey, B. S., *Mechanics of fluids*, 6<sup>th</sup> ed., Chapman and Hall, 1989, London, UK.
- [15] Balland, S., Fernandez Villace, V. and Steelant, J., "Thermal and Energy Management for Hypersonic Cruise Vehicles – Cycle Analysis", *20<sup>th</sup> AIAA International Space Planes and Hypersonic Systems and Technologies Conference*, Glasgow, UK, 2015.  
<https://doi.org/10.2514/6.2015-3557>
- [16] Langener, T., Erb, S. and Steelant, J., "Trajectory simulation and optimization of the LAPCAT-MR2 hypersonic cruiser concept", *29<sup>th</sup> Congress of the International Council of the Aeronautical Sciences*, St. Petersburg, RU, 2014.
- [17] Rodriguez-Segade, M., Hernandez, S., Diaz, J., Baldomir, A. and Lopez, D., "Structural scheme for the propulsion systems and the complete hypersonic STRATOFly vehicle", *AIAA Scitech 2020 Forum*, Orlando, FL, 2020.  
<https://doi.org/10.2514/6.2020-1107>
- [18] Scigliano, R., De Simone, V., Marini, M., Roncioni, P., Fusaro, R. and Viola, N., "Preliminary Finite Element Thermal Analysis of STRATOFly Hypersonic Vehicle", *23<sup>rd</sup> AIAA International Space Planes and Hypersonic Systems and Technologies Conference*, Montreal, CA, 2020.  
<https://doi.org/10.2514/6.2020-2422>
- [19] Fusaro, R.; Gori, O., Ferretto, D.; Viola, N., Roncioni, P. and Marini, M., "Integration of an increasing fidelity aerodynamic modelling approach in the conceptual design of hypersonic cruiser", *32<sup>nd</sup> Congress of the International Council of the Aeronautical Sciences*, Shanghai, CN; 2021.
- [20] Rachov, P., Hernan, T. and Lentini, D., "Electrical feed systems for liquid propellant rocket engines", Department of Electronic Sciences, University of Buenos Aires, Buenos Aires, AR, 2010  
<https://doi.org/10.13140/2.1.4431.9042>
- [21] American National Standards Institute "Mass Properties Control for Space Systems", ANSI/AIAA S-120A-201X, 2015
- [22] Cheng, K., Qin, J., Sun, H., Dang, C., Zhang, S., Liu, X. and Bao, W., „Performance assessment of an integrated power generation and refrigeration system on hypersonic vehicles”, *Aerospace Science and Technology*, Vol. 89, 2019, pp. 192-203.  
<https://doi.org/10.1016/j.ast.2019.04.006>
- [23] Cheng, K., Qin, J., Sun, H., Dang, C., Zhang, S., Liu, X. and Bao, W., „Performance assessment of a closed-recuperative-Brayton-cycle based integrated system for power generation and engine cooling of hypersonic vehicle”, *Aerospace Science and Technology*, Vol. 87, 2019, pp. 278-288.  
<https://doi.org/10.1016/j.ast.2019.02.028>